Journal of Water Process Engineering 56 (2023) 104294

Contents lists available at ScienceDirect

Journal of Water Process Engineering

journal homepage: www.elsevier.com/locate/jwpe

An investigation on the removal of tramadol analgesic in deionized water and final wastewater effluent using a novel continuous flow dielectric barrier discharge reactor

Samuel O. Babalola, Michael O. Daramola, Samuel A. Iwarere *

Department of Chemical Engineering, Faculty of Engineering, Built Environment and Information Technology, University of Pretoria, Hatfield 0028, Pretoria, South Africa

ARTICLE INFO

Keywords:
Tramadol
Wastewater effluent
Dielectric barrier discharge
Reactive species
Degradation efficiency

ABSTRACT

In this study, the degradation of tramadol (TRA) was studied for the first time in deionized water (D·I) and final wastewater effluent (FWWE) using a dielectric barrier discharge reactor operated in a continuous flow mode. Initially, the reactor was optimized for voltage and initial concentration conditions. After 60 min treatment, the degradation efficiency of TRA was 93 % in D·I and only 27 % in FWWE. Also, the pseudo-first-order rate constant in D·I (0.056 min^{-1}) was an order of magnitude higher than the FWWE (0.0056 min^{-1}). To understand the reasons for this disparity, experiments were conducted to investigate the impact of conductivity, pH, and certain natural radical scavengers present in the wastewater. The results revealed that the rate of degradation and kinetics of TRA in the presence of HCO_3^- was comparable to those observed in FWWE due to the scavenging of the $^{\bullet}OH$ radicals. Meanwhile, Fenton reaction with TRA was confirmed with the synthetic solution based on the increased production of H_2O_2. Toxicity tests showed that the treated TRA solution did not inhibit the growth of *Escherichia coli* as opposed to the untreated solution.

1. Introduction

The occurrence of residual pharmaceuticals in the water cycle has been linked to their increased production, consumption, and decrease in their prices over the last two decades [1]. Although they are detected in very low concentrations (ngL^{-1} and μgL^{-1}), these emerging contaminants have become a concern to both the scientific community and the public due to their persistence in the environment and toxicity reports [2]. One of the pharmaceutical compounds of interest is Tramadol (TRA), an opioid that is widely used for treating moderate to severe pains. Its global consumption surged from 290 tons in 2006 to 424 tons in 2012 [3], with Germany alone prescribing 24 tons in 2012 [4]. Meanwhile, only about 70 % of TRA dosage is metabolized by the human system, leaving the remaining 30 % to be excreted as waste [5]. Given its high hydrophilicity and low biodegradability, TRA has been classified as one of the extremely recalcitrant water micropollutants [6]. This characteristic renders its elimination through conventional wastewater treatment setups very challenging. Furthermore, documented reports have surfaced detailing the adverse impacts of TRA on aquatic life, including Zebra fish [7], Crayfish [8], Tilapia [9], Common carp [10], among others. These findings underscore the urgency for the development of technologies that can effectively deal with the micropollutant in water sources.

Various methods have been proposed to address the challenge of recalcitrant micropollutants like pharmaceuticals in water, with advanced oxidation processes (AOPs) gaining more attention in recent times [11–13]. These innovative methods encompass the generation of highly potent reactive species such as ozone (E_0: 2.07 V) and hydroxyl radicals (E_0: 2.8 V), that can potentially oxidize toxic pharmaceutical compounds into harmless by-products [14]. Hydroxyl radicals ($^{\bullet}OH$) are particularly desirable because they are not only strong oxidizers but also non-selective towards various types of micropollutants. A variety of AOPs, such as ozonation [15], ozone-assisted process with Fe [16], ultraviolet irradiation with chlorine and H_2O_2 [17], photocatalysis [18–20], Fenton-like process [21] have demonstrated successful TRA degradation with notable removal efficiencies. Among emerging AOPs, non-thermal plasma technology (NTP) has garnered significant interest due to its simplicity, versatility, high energy efficiency, environmental suitability, and minimal reliance on additional chemical reagents. NTP treatment capitalizes on the synergy of reactive species – ($H^{\bullet}$, $^{\bullet}OH$, $O^{\bullet}$, $^1O_2$), molecules (H_2O_2, O_3, etc.), ultraviolet light, and shock waves [22]. Within NTP configurations, the Dielectric barrier discharge (DBD)

* Corresponding author.
E-mail address: samuel.iwarere@up.ac.za (S.A. Iwarere).

https://doi.org/10.1016/j.jwpe.2023.104294
Received 10 July 2023; Received in revised form 4 September 2023; Accepted 11 September 2023
Available online 16 September 2023
2214-7144/© 2023 The Authors. Published by Elsevier Ltd. This is an open access article under the CC BY license (http://creativecommons.org/licenses/by/4.0/).

stands out for its operation at low/atmospheric pressure conditions and near-ambient temperatures. This configuration offers distinct advantages such as low energy consumption, thereby contributing to a cost-effective treatment solution. Alternate NTP configurations for water treatment have been reported by Cui et al. [23], and their efficiencies have been extensively discussed by Malik [24].

Several factors affect the effectiveness of an AOP in eliminating micropollutants, including the mode of operation (batch, continuous, etc), solution conductivity, and the presence of natural radical scavengers, among others. Typically, studies on TRA removal have been conducted in batch mode where the generated reactive species have adequate mass transfer in the solution and contact with the pollutant. While this mode yields rapid and energy-efficient degradation, its drawback lies in limited throughput, curtailing potential applicability beyond the laboratory-scale [25]. Also, the conductivity of the solution can influence the rate of reactive species generated in certain AOPs. While a Surface Dielectric Barrier Discharge (SDBD) reactor remains unaffected by water conductivity because the discharge has no direct contact with the liquid [26], initiating a discharge in a Volume Dielectric Barrier Discharge (VDBD) system necessitates low conductivity in the order of a few μS/cm [27]. Elevated solution conductivity in VDBD systems reduces the length of the discharges, thereby decreasing the intensity of the reactive species generated and ultimately impacting pollutant degradation. For instance, Karoui et al. [28] observed varying degradation efficiencies for ciprofloxacin across various water matrices: ultra-pure water (15.12 μS/cm), tap water (492.2 μS/cm), and pharmaceutical water (2454 μS/cm) in a VDBD treatment. The degradation efficiencies observed were 100 %, 76 %, and 60 %, respectively. Also, natural ions in raw aqueous solutions are acknowledged as potential scavenger for the reactive species. These dynamics elucidate the rationale behind majority of DBD studies concentrating on solutions characterized by low conductivity and high purity. However, there are unanswered questions on how the degradation of micropollutants are prohibited in real wastewater effluent.

Therefore, this study not only examined the performance of a flow-through VDBD-type reactor in the degradation of TRA but also probes the divergences in pollutant removal between synthetic water and final wastewater effluent. To date, micropollutant investigations in this specific context remain scarce, prompting the development of multiple assumptions in this study. The first hypothesis was based on the influence of solution property, particularly the conductivity of the wastewater effluent, given its potential to affect the length of the discharges as mentioned earlier. The second hypothesis considered the influence of cross-interference reactions between natural ions (Cl^-, HCO_3^-) and the ROS generated by the reactor. The influence of naturally occurring ions in the wastewater effluent was used in elucidating their impact on the reactive species available for contaminant degradation. Finally, a simple toxicity investigation was performed with *Escherichia coli*.

2. Experimental method

2.1. Materials

Tramadol hydrochloride ($C_{16}H_{25}NO_2$.HCl, purity >99 %) was purchased from Sigma-Aldrich Co. (Johannesburg, South Africa). The molecular structure of this compound is shown in Fig. S1. Sodium hydroxide (NaOH), sulphuric acid (H_2SO_4), potassium chloride (KCl), and sodium chloride (NaCl) were purchased from Glassworld (Johannesburg, South Africa). Other chemicals like Sodium hydrogen carbonate ($NaHCO_3$), and Iron (II) sulphate heptahydrate ($FeSO_4.7H_2O$) were supplied by Merck Chemicals (PTY) Ltd. (Germiston, South Africa). All the chemicals were used without further purification because of their high purity. The synthetic TRA solutions were prepared in deionized water which had a resistivity of about 18.2 MΩ/cm. Final wastewater effluent was collected from a local municipality in Pretoria West, South Africa, at the effluent discharge point.

2.2. Experimental procedure

5 mg/L TRA solution was prepared in a litre of deionized water, final wastewater effluent, and in solutions containing NaOH (2 M), H_2SO_4 (2 M), NaCl (2 mg/L), $NaHCO_3$ (236 mg/L), KCl (0.3 M), $FeSO_4.7H_2O$ (2 mg/L). These solutions were subjected to plasma treatment individually. The experimental setup, shown in Fig. 1(a), featured a DBD plasma reactor composed of borosilicate glass with wall thickness and outer diameters of 0.23 cm and 4 cm, respectively. The length of the glass tube is 30 cm, and it incorporated a stainless-steel rod of 1.27 cm in diameter and 29 cm in length, serving as the high-voltage (HV) electrode. A conductive copper tape, 1 mm width, and 0.1 mm thickness constituted the ground electrode, encircling the glass both radially and laterally as shown in Fig. 1(b). Air was introduced naturally into the reactor as the working gas without an aerodynamic device. The plasma discharge was initiated and maintained by an alternating current (AC) power source (built by Jeenel Technologies Pty, Boksburg, South Africa) operated between 6 and 8 kV input voltage and a constant frequency of 20 kHz. According to Fig. 1(a), the high voltage line was connected to the HV multi-pin inner stainless-steel electrode, positioned centrally within the reactor. The HV electrode was hollow, facilitating the passage of water from the storage into the reactor, while the discharges are generated at the multi-pin edges. The contaminated water was sprayed out evenly at the upper section of the reactor through a micro jet spray positioned in a spacer at the top of the HV electrode. The spacer also helps to hold the electrode centrally within the reactor. As the water descended, it contacts the purple-coloured discharges at the multi-pin edges, subsequently flowing back into the storage. This cyclic process persisted for the designated treatment duration, with the water being pumped back into the reactor using a peristaltic pump operated at 400 mL/min flow rate. To ensure uniform solution mixing in the storage container, a magnetic stirrer was employed. Additionally, the pH of the solution was adjusted with aqueous NaOH and H_2SO_4 solutions.

Unless otherwise specified, the input voltage from the AC power supply was set at 8 kV, while the actual discharge current and voltage measurements were monitored with a digital oscilloscope (Rigol DS1074 Zplus, 70 MHz GSa/s). The dissipated power for the reactor was calculated via Eq. (1) [26]. Optical emissions spectra were captured with a spectrometer (manufactured by StellarNet Inc) to investigate the reactive species generated in the DBD reactor.

$$P\,(W) = \frac{I}{T}\int_0^T V(t) \times I(t)dt \tag{1}$$

where P is the average dissipated power, while V(t) and I (t) are the waveforms of voltage and current at time t, respectively.

2.3. Analytical measurements

The pH and conductivity of the solution were measured with a HANNA Multiparameter HI98194 meter. The concentration of hydrogen peroxide and ozone were obtained by spectrophotometry using a Lovibond® Spectrodirect water testing instrument (Tintometer® Group, Germany) after the contaminated solution was exposed to plasma treatment. To achieve this, each of the reagents assigned to the different molecules were added to the samples withdrawn from the storage in a designated vial without dilution. The removal of TRA was monitored by measuring TRA concentration as a function of time during plasma treatment. To achieve this, 1 mL aliquot of the treated solution was withdrawn from the storage at 5 min intervals and analyzed on a High-Performance Liquid Chromatography (HPLC). The HPLC used is an Alliance Waters 2695 with a UV–Vis Waters detector equipped with Waters C18 5 μ column which has 4.6 by 250 mm dimensions. The mobile phase used consisted of 50 % acetonitrile and 50 % water (with 1 % acetic acid) at a flow rate of 1 mL/min. The injection volume was set at 10 μL while the UV detector was operated at 272 nm. TRA

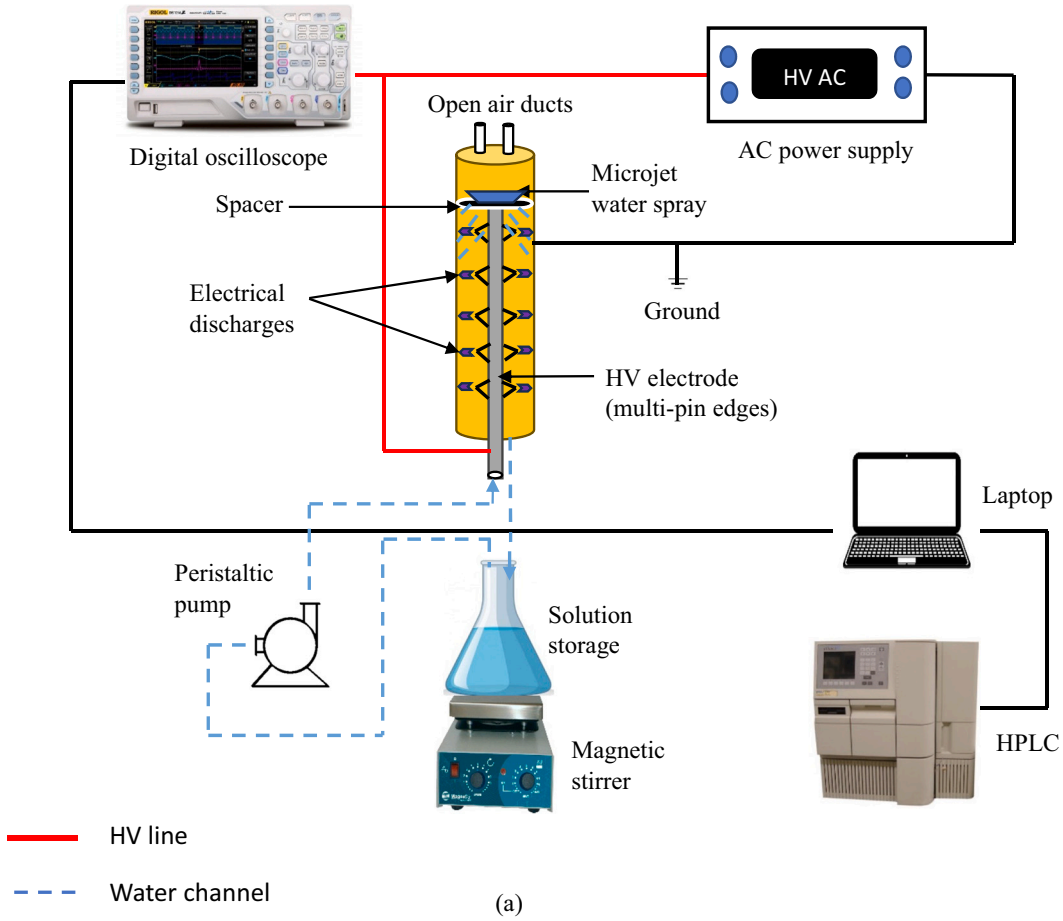

Fig. 1. Experimental arrangement for the tramadol degradation process (a) schematic illustration of the setup (b) DBD plasma reactor showing purple streamer discharges at the edges of the multi-pin electrode.

degradation efficiency in the solution was estimated using Eq. (2):

$$\eta(\%) = \frac{(TRA_o - TRA_t)}{TRA_o} 100 \quad (2)$$

Meanwhile, TRA degradation kinetics was confirmed as pseudo first-order according to Eq. (3):

$$In\left(\frac{TRA_o}{TRA_t}\right) = kt \quad (3)$$

TRA_o and TRA_t (mg) represent the initial tramadol concentration and concentration at a predetermined time, t(min), respectively. η represents tramadol degradation efficiency and the rate constant is defined as k (min^{-1}). All inorganic ions present in the water matrices were quantified using a 940 professional Ion Chromatography (IC) variable chromatography (Metrohm, Switzerland), with a Metrosep C6–250/4.0 separation column and C6 eluent 8 mM oxalic acid (Metrohm, Switzerland). Also, the energy yield, Y (g/kWh), is defined as the amount of TRA decomposed per unit of energy consumed. This was calculated with Eq.

(4) [26]:

$$\Upsilon(g/kWh) = \frac{TRA_o \times V \times \frac{\eta}{100}}{P \times t} \quad (4)$$

where V is the volume of the treated water (L), η the degradation efficiency (%), P is the average power dissipated in the DBD reactor (W) and t represents the treatment time (h). Υ_η describes the energy yield at a specific degradation efficiency, η (%).

To investigate the toxicity of the solution, an American Type Collection strain of Gram-negative *Escherichia coli* (ATCC 10536™) was purchased from Sigma Aldrich (Johannesburg, South Africa), and grown on Luria Bertani (LB) medium under incubation conditions for batch-batch reproducibility. The antibacterial activity of plasma-treated and untreated solutions containing TRA was tested by diffusion bioassay to determine zones of inhibition. Prior to the toxicity investigation, the bacterium was inoculated in nutrient broth at 37 °C for 24 h after which it was overlaid on the surface of nutrient agar plates. The tests were conducted in triplicate for untreated, plasma-treated TRA solutions respectively, and a control. After incubation, the presence of inhibition zones was used to confirm antibacterial activity.

3. Results and discussion

3.1. Electrical and optical characteristics of the dielectric barrier discharge reactor

The electrical properties of a plasma system directly influence its degradation efficiency. Therefore, voltage and current the variations during plasma discharge were captured with the digital oscilloscope and used in the calculation of the dissipated power. Fig. S2 provides the characteristic current-voltage waveforms of the gas-liquid DBD plasma discharges with air. As shown, the peak value of discharge voltage and current were approximately 8.0 kV and 44.8 mA. In this study, the average dissipated power was estimated as 77 W.

To understand the reaction mechanism facilitated by the reactive species present, emission spectroscopy was conducted on the plasma generated as presented in Fig. 2 in a range of 270–450 nm and 600–850 nm. Each specie was identified by comparing the peak positions with the atomic line database obtained in literature references [14, 29, 30]. As expected in atmospheric air non-equilibrium discharges, the spectra were dominated by the excited N_2 molecules, then N_2^+, OH, and O. These were generated primarily by energetic electron collisions with N_2, O_2, and H_2O molecules [30]. The N_2 spectrum ($C^3\Pi_u - B^3\Pi_g$) was followed by the N_2 spectrum ($B^3\Pi_g - A^3\sum_u^+$), indicating the formation of N_2 ($A^3\sum_u^+$) states. According to Lu et al. [31], N_2 ($B^3\Pi$ and $C^3\Pi$) and N_2^+ ($x^2\sum_g^+$) states are products of the electron impact excitation of the molecular ground state N_2 ($x^1\sum_g^+$). Meanwhile, OH radicals found at 297 and 309 nm [29] could be formed by the dissociation of water molecules caused by an electronic impact, as described in Eq. (5). Whereas O radicals at 777 nm might have been formed by energetic collisions of electrons with O_2 molecules, as described in Eq. (6) [32].

$$H_2O + e^- \rightarrow \dot{H} + \dot{O}H + e^- \quad (5)$$

$$O_2 + e^- \rightarrow 2\dot{O} + e^- \quad (6)$$

The analysis of the optical emission spectra revealed the generation of nitrogen, hydroxyl radicals, and atomic oxygen in the DBD reactor. These active species were found to be transferred into the liquid phase, where they further facilitated the production of secondary oxidative species, including H_2O_2, O_3, NO_3, and NO_2 within the aqueous solution.

3.2. Influence of operating conditions on the removal TRA

Initially, the impact of applied voltage and initial concentration on TRA degradation efficiency was assessed. The parameters yielding the highest TRA conversion were subsequently considered as the optimal conditions.

3.2.1. Effect of input voltage

The input voltage is one of the significant parameters showing a great influence on the degradation of micropollutants with DBD reactors [33]. An increase in the input voltage is expected to increase the concentration of the reactive species formed in the reactor which will simultaneously increase the rate of degradation of the pollutant. From the results in Fig. 3(a), as the voltage increased from 6 to 8 kV, the rate of conversion of TRA also increased from 71 % to 93 % respectively during the plasma treatment. Similarly, the reaction kinetics more than doubled from 0.022 to 0.056 min^{-1} respectively, as shown in Fig. S3. This confirms that there is a positive relationship between the applied voltage and the rate of the reaction for TRA degradation with the DBD reactor. Comparable observations surfaced during the plasma-induced removal of pharmaceuticals like cephalosporins [34], Ibuprofen [35] among others.

During the initial 20-min period, the degradation of TRA at 8 kV and 7 kV voltage inputs proceeded rapidly reaching 81 % and 73 % conversions respectively. Conversely, the rate of conversion was lower 6 kV. However, after 20 min, TRA degradation at 6 kV showed a consistent linear trend, while at 7 kV and 8 kV, the degradation proceeded at a notably slow rate. This divergence could potentially stem from a decline in available reactive species over extended durations. Another plausible

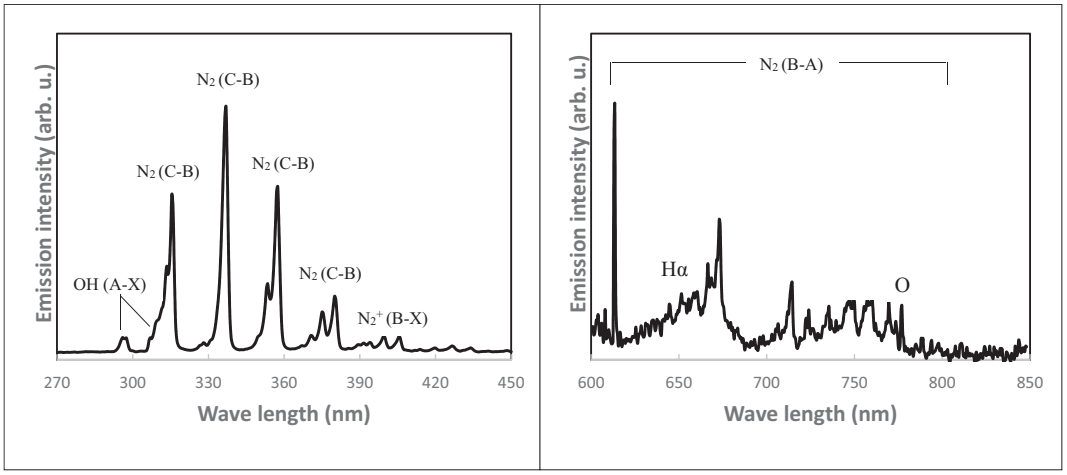

Fig. 2. Optical emission spectrum of the plasma generated in the dielectric barrier discharge reactor at 20 kHz and 8 kV.

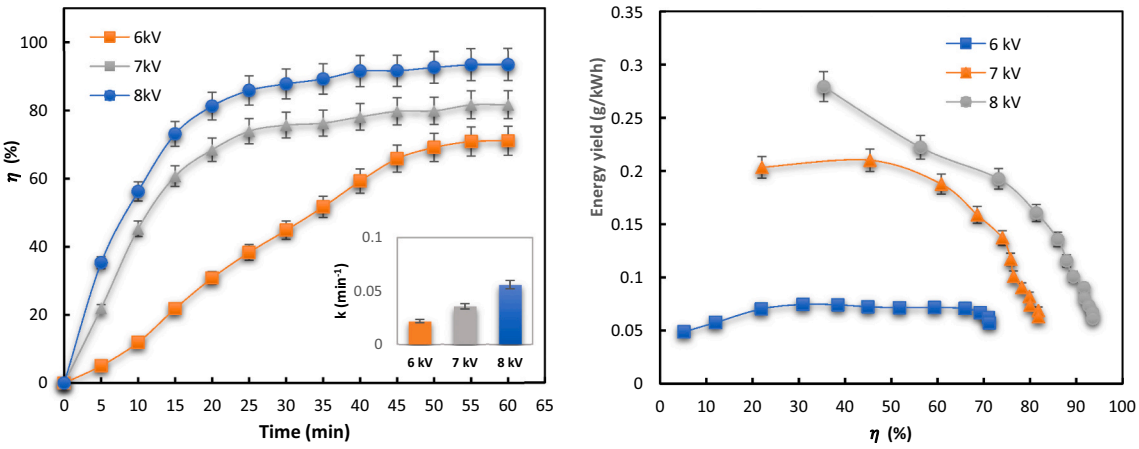

(a) (b)

Fig. 3. Effect of voltage on 5 mg/L TRA degradation. (a) Degradation efficiency and kinetics. (b) Energy yield.

explanation is the heightened competition between TRA and its intermediate products for the reactive species at 7 kV and 8 kV. Thus, the impact of applied voltage after 20 min on the removal of the actual contaminant was limited. Furthermore, the energy yield for TRA increased with the applied voltage as shown in Fig. 3(b). For example, at 50 % TRA degradation, the energy yield (Y_{50}) computed at 6 kV, 7 kV, and 8 kV was approximately 0.07 g/kWh, 0.2 g/kWh, and 0.23 g/kWh, respectively. For each voltage, the energy yield decreased with an increase in the rate of TRA degradation. This is because, under a constant input voltage, the degradation rate of the target pollutant increases up to a point in which further energy input no longer contributes to pollutant removal.

The performance of the DBD plasma used in this work was compared with other AOPs in Table 2. As mentioned earlier, most of the studies were conducted in batch modes with small solution volumes. A commercialized pulsed corona discharge reactor used in the degradation of TRA achieved 91 % degradation efficiency of the contaminant in 2 h [36]. Photocatalysis experiments conducted in 25 mL TRA solution gave 81.1 % and 90.63 % degradation efficiencies in 80 min and 120 min with bismuth ferrite and cobalt doped-bismuth ferrite catalysts, respectively.

3.2.2. *Effect of initial concentration*

Using the optimum voltage of 8 kV, the effect of initial concentration on the degradation of TRA was examined. The results provided in Fig. 4 (a) showed that the degradation efficiency of the pollutant decreased from 93 % to 11 % with an increase in the initial concentration from 5 mg/L to 20 mg/L. Similarly, the reaction kinetics reduced from 0.056 to 0.002 min^{-1}, respectively, as shown in Fig. S3. This result can be explained by the increase in the molecules of TRA caused by an increase in its initial concentration. As TRA molecules increase, not only does the consumption of the reactive species intensifies, but cross-reactions between the intermediate products and the reactive species also escalates. This limits further degradation of the pollutant itself. It is noteworthy that the concentration of TRA considered in this study surpasses what is typically encountered in the environment [38]. This suggests that at a much lower initial concentration of TRA than what was reported in this study, the degradation efficiency with our DBD system will be higher. Fig. 4(b) shows that at lower degradation efficiencies, the energy yield

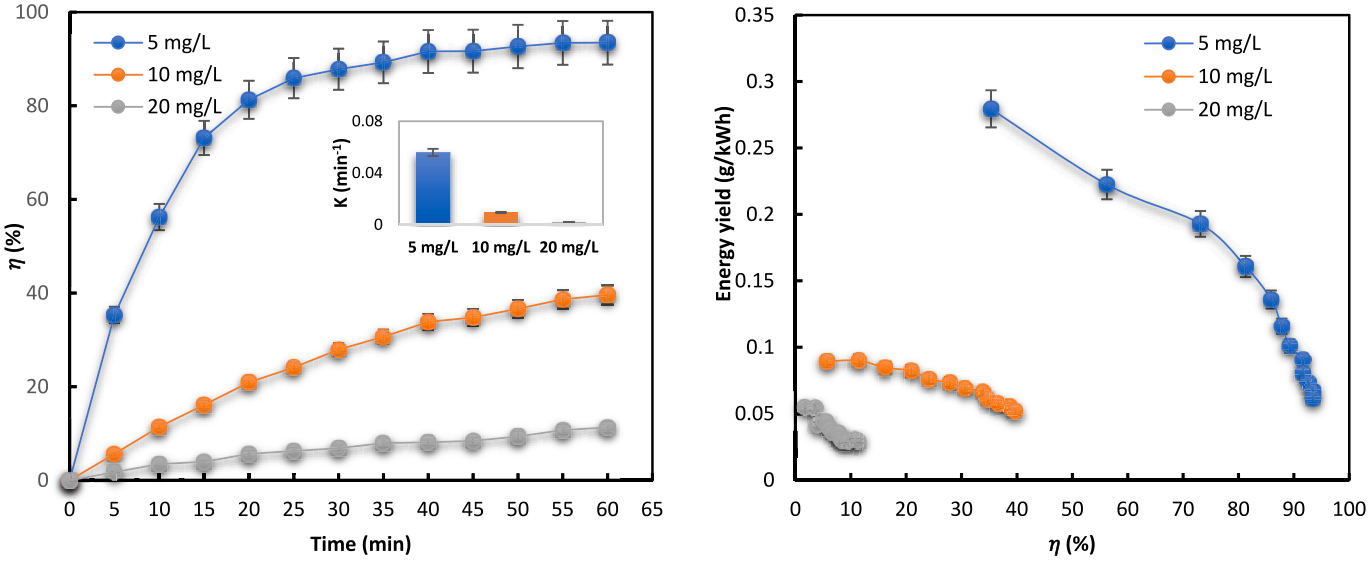

(a) (b)

Fig. 4. Effect of concentration on TRA degradation at 8 kV. (a) Degradation efficiency and kinetics. (b) Energy yield.

decreased as the initial concentration increased. A similar observation was reported for the removal of sulfadiazine antibiotics in water [39].

3.3. Contribution of active species: generation of O_3, H_2O_2, NO_3^- and NO_2^- during the DBD discharge

The production of secondary oxidative species like ozone, hydrogen peroxide, nitrate and nitrite were examined in this study. Among these, the reactive oxygen species (O_3 and H_2O_2) have received significant attention due to their pivotal role in oxidizing micropollutants. The production of O_3 is based on Eq. (7), as derived from Eqs. (5) and (6), while H_2O_2 is produced according to Eqs. (8)–(9), respectively.

$$O + O_2 \rightarrow O_3 \quad (7)$$

$$OH + \dot{O}H \rightarrow H_2O_2 \quad (8)$$

$$H + \dot{H}O_2 \rightarrow H_2O_2 \quad (9)$$

During the initial 20 min treatment period, the concentration of both O_3 and H_2O_2 increased simultaneously under the air-plasma treatment, with H_2O_2 having more presence in the solution and reaching as high as 2.2 mg/L. However, over extended durations, a sharp decline in the concentration of H_2O_2 was observed plummeting to as low as 0.24 mg/L after 1 h. The decline in the concentration of H_2O_2 provides another important explanation for the degradation rate of TRA after 20 min as seen in Fig. 5(a). This is because H_2O_2 is a direct product of the combination of short-lived OH radicals. Therefore, a decrease in its concentration means that less •OH is generated within the plasma. The generation of O_3, on the other hand, quadrupled within the first 20 min of TRA removal and subsequently diminished. This result also verifies that O_3 played an important role in the elimination of TRA. Fig. 5(b) shows that the concentration of NO_3^- in the solution increased from 10 mg/L in the first 22 min to 76 mg/L after an hour, while NO_2^- increased from 4.8 mg/L in the first 30 min then decreased to 4.05 mg/L after an hour. An increase in the concentrations of the reactive nitrogen species in the solution will potentially increase acidity, especially in the absence of a pH buffer.

3.4. Comparison of the degradation of TRA in deionized water and final wastewater effluent

Based on the optimum initial concentration and voltage obtained, the degradation of TRA in deionized water and final wastewater effluent matrices was compared as shown in Fig. 6(a). After an hour of plasma treatment, the degradation efficiency of TRA was only 27 % in the wastewater compared to 93 % observed in deionized water. Also, the rate constant for TRA degradation in FWWE was 0.0056 min^{-1} which is an order of magnitude lower than that of the D·I matrix. The maximum energy yield was also markedly different, with the D·I yielding 0.28 g/kWh and the effluent matrix showing only 0.02 g/kWh, as illustrated in Fig. 6(b).

The pH and conductivity variations within the solution matrices during treatment are illustrated in Fig. 6(c). During the initial 5 min of treatment, the pH of the synthetic TRA solution decreases rapidly then continued at a steady value of about 0.11 in the next 55 min. This observation can be attributed to the increased formation of nitrogen ions (NO_3^- and NO_2^-) within the solution as described in Fig. 5(b). The presence of NO_3^- and NO_2^- ions in the solution enables the formation of HNO_3 and HNO_2 compounds, subsequently resulting in increased acidity. Also, an increased formation of ions can be directly correlated with the linear increase in the conductivity of the solution as illustrated in Fig. 6(c). This further imposes limitations on the continued degradation of TRA. The presence of nitrogen ions and increased solution acidity may be attributed to the use of atmospheric air plasma system, as opposed to pure synthetic oxygen gas for plasma generation [34]. On the other hand, the pH of the wastewater solution remained fairly constant, while the conductivity only increased slightly. This is largely due to the buffering properties of the carbonate ion present in the wastewater effluent.

To examine the other factors responsible for the disparity in the degradation of TRA in the water matrices, some hypotheses were made. Firstly, considering that the wastewater effluent had a conductivity of more than two orders higher than deionized water (2 μS/cm) in magnitude, we hypothesized that conductivity might potentially influence the degradation of TRA in the wastewater. To verify this, KCl was added to the deionized TRA solution to increase its conductivity to that of wastewater (548 μS/cm). From the result provided in Table S1, the degradation rate constant at this result (0.0036 min^{-1}) defers from that of the final wastewater effluent (0.0056 min^{-1}). These results suggest that conductivity was not the sole determinant of the disparity. To further investigate other possible limiting factors, control experiments were conducted for TRA in deionized water to examine (i) the effect of chloride ions, as chlorine is always used at the disinfection stage before final effluent discharge, (ii) the effect of carbonate ions, as sodium bicarbonate salts are added during treatment procedures to control pH. (iii) An in-depth investigation of the effect of pH variations was also conducted. Furthermore, a possible effect of the Fenton reaction, linked to the presence of Fe^{2+} ion was explored, despite their absence in the wastewater based on Table 1.

3.4.1. Effect of chloride ions

Following the investigation into conductivity, the subsequent aspect explored was the potential influence of chloride ions. Chloride ions are primarily introduced intoe wastewater via hypochlorite chemicals, often

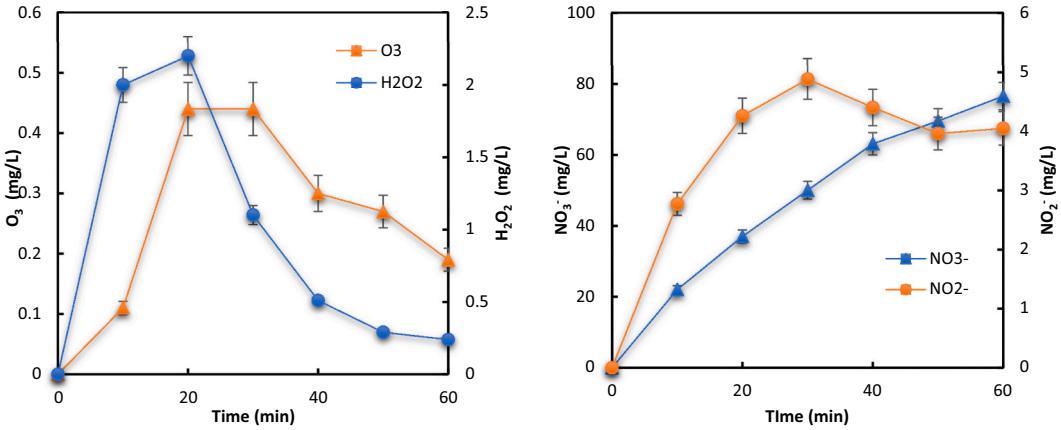

Fig. 5. Reactive species formed during TRA degradation (5 mg/L initial concentration and 8 kV). (a) O_3 and H_2O_2 concentration. (b) NO_3^- and NO_2^- concentration.

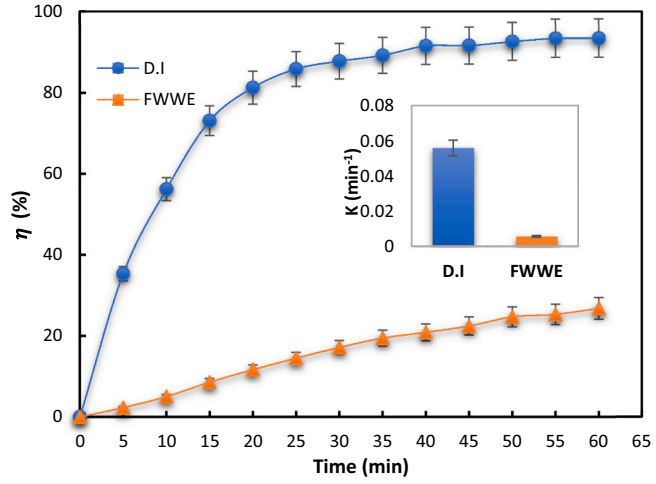

(a)

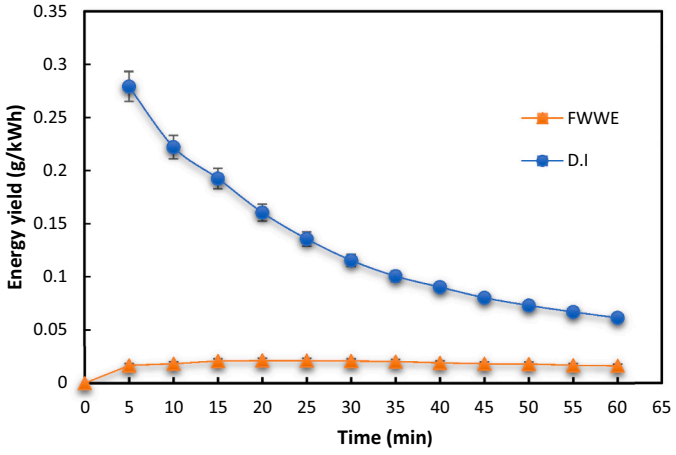

(b)

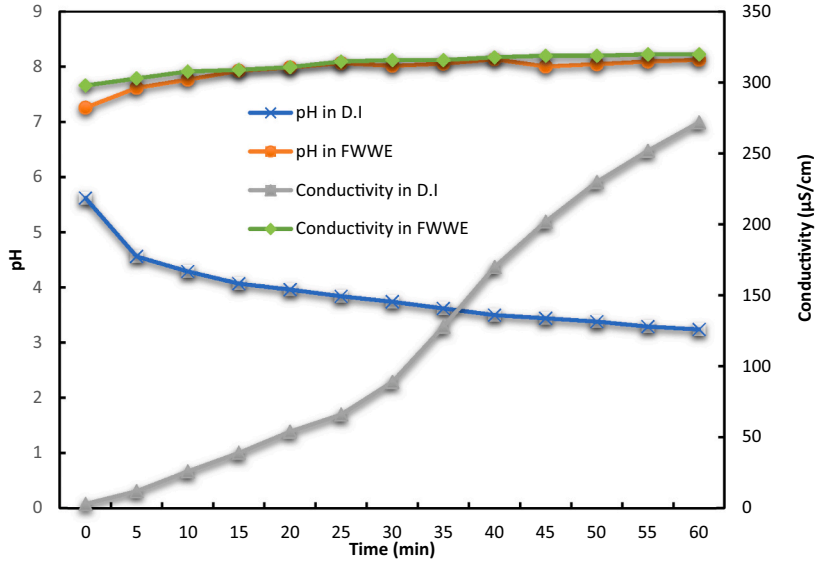

(c)

Fig. 6. (a) Degradation of tramadol in deionized water and final wastewater effluent as a function of time; (b) energy yield comparison (c) pH and conductivity of the solution matrices as a function of time (initial TRA concentration: 5 mg/L; voltage: 8 kV).

Table 1
Ion chromatography analysis of the final wastewater effluent obtained from Daspoort Municipality, South Africa.

Parameter	Unit	Measured value
Active hydrogen ions (pH)		7.53
Conductivity	μS/cm	548
Total suspended solid (TSS)	mg/L	10.4
Chemical oxygen demand	mg/L	10
Ortho-phosphate	mg/L	0.06
Chloride	mg/L	56.26
Sulphate	mg/L	95.52
Nitrite	mg/L	1.42
Nitrate	mg/L	12.40
Iron	mg/L	0
Bicarbonate	mg/L	236
Lithium	mg/L	0.03
Sodium	mg/L	58.24
Manganese	mg/L	0.52
Magnesium	mg/L	24.74
Bromide	mg/L	5.42
Calcium	mg/L	44.43

used at the final effluent treatment phase for microbial disinfection. According to Table 1, the concentration of chloride ions measured in the wastewater was 56.26 mg/L. Therefore, to investigate the effect of chloride ions, 92.9 mg of sodium chloride was added into a deionized TRA solution and subjected to an hour of plasma treatment. The results, as depicted in Fig. 7, revealed that the degradation of TRA in wastewater and TRA in D·I with sodium chloride exhibited similar trend during the initial 25 min. Subsequently, the degradation of TRA in D·I with sodium chloride continued linearly up to 52 % efficiency. Table S1 showed that the final rate constant for the TRA with chloride ions was almost double that of the final wastewater effluent. Therefore, while the addition of chloride ions initially impacted TRA degradation similar to the trend observed in the wastewater, it does not completely elucidate the observations for TRA in the effluent reaction medium. This is because chlorine gas (E_0: 1.36 V) also has the potential to oxidize TRA in the solution. Another study has reported that the addition of chlorine to a UV system improved the removal efficiency of TRA in just 10 min compared to UV/H_2O_2 [17]. The interaction between chloride ions and •OH is explained in Eqs. (10)–(13) [40]. However, the presence of NaCl as a chloride source was reported to harm the degradation efficiency of dye [41], due to the abstraction of •OH radicals.

$$NaCl \rightarrow Na^+ + Cl \quad (10)$$

$$Cl + \dot{O}H \rightarrow HOCl \quad (11)$$

$$Cl + \dot{O}H \rightarrow Cl + \dot{O}H \quad (12)$$

$$Cl + Cl \dot{\rightarrow} Cl_2 \quad (13)$$

3.4.2. Effect of bicarbonate ions

The concentration of bicarbonate ions in the wastewater was 236 mg/L as provided in Table 1. To examine the influence of this potential radical scavenger on TRA degradation, 325 mg of $NaHCO_3$, equivalent to the concentration of the ion in the wastewater, was added to TRA deionized water solution. The solution was then subjected to an hour plasma treatment. The results obtained are provided in both Fig. 7 and Table S1. In comparison with the wastewater dataset, these results revealed identical values for both degradation efficiency (27 %) and rate constant (0.0056 min^{-1}). This implies that the presence of bicarbonate ions in the FWWE primarily accounts for its diminished degradation efficiency. However, this observation may be different for other organic compounds and different water matrices. For instance, a study reported that the presence of bicarbonate ions in tap water improved the degradation efficiency of phenol compared to a deionized (Milli-Q) water matrix [42]. In this case, the carbonate radical (CO_3^{-}•) generated appeared to be a good oxidizing agent for phenol. Meanwhile, CO_3^{-}• is known to have a longer half-life than •OH [43]. The oxidation of some selected organic compounds has also been found to be facilitated by the presence of CO_3^{-}• [44]. In this present study, bicarbonate ions scavenged the hydroxyl radicals generated by the DBD plasma reactor which was the primary specie responsible for TRA degradation. CO_3^{-}• was generated according to Eq. (14) [45].

$$HCO_3^- + \dot{O}H \rightarrow CO_3^{-\cdot} + H_2O \quad (14)$$

Also, despite the nitric compounds present in the solution, the pH recorded in Table S1 remained constant for the bicarbonate reaction solution. As explained earlier, the presence of bicarbonate ions in the solution helps to stabilize and maintain the pH level.

3.4.3. Effect of pH

The impact of pH on TRA degradation was examined by adding H_2SO_4 and NaOH to the deionized water matrix to adjust the pH levels. The experiments were carried out at pH levels of 3, 7, and 11, respectively, and compared with TRA deionized water solution. According to the results provided in Fig. S4, an increase in pH reduces the rate of the reaction and consequently the efficiency of tramadol removal with the DBD reactor. Also, the reaction is unfavourable at extremely low pH values like 2. Meanwhile, a study on the removal of sulfadiazine with DBD reported that the degradation efficiency of the contaminant

Table 2
Degradation of TRA in water with selected AOPs.

Methods	Operating conditions	Mode	Degradation efficiency	Treatment time	Rate constant	References
Pulsed corona discharge	33.4 μM TRA prepared in 10 L and pH 6	Continuous flow	91 %	120 min	3.10 $m^3\ kW^{-1}\ h^{-1}$	[36]
Photocatalysis	10 mg/L TRA with 100 mg/L TiO_2 catalyst	Batch	95 %	20 min	0.153 min^{-1}	[18]
Electro-Fenton	26.3 mg/L TRA in 250 mL solution at 500 mA	Batch	100 %	10 min	5.59 × 10^9 $M^{-1}\ s^{-1}$	[21]
Photocatalysis	Bismuth ferrite in 25 mL TRA solution	Batch	81.1 %	120 min	0.0145 min^{-1}	[20]
	cobalt-doped bismuth ferrite in 25 mL TRA solution		90.63 %	80 min	0.0329 min^{-1}	
	Fe_2O_3 phosphotungstic acid in 25 mL TRA solution		91.32 %	80 min	0.0312 min^{-1}	
UV/Chlorine	5 μg/L TRA in 25 mL solution buffered to pH 7	Batch	100 %	10 min	0.3785 min^{-1}	[17]
UV/H_2O_2	5 μg/L TRA in 25 mL solution buffered to pH 7		100 %	15 min	0.2005 min^{-1}	
Gamma irradiation combined with nanofiltration	20 mg/L TRA in ultrapure water with 5 kGy	Batch	100 %	12 min	–	[37]
Electrochemical oxidation	100 μM TRA in 100 mL under 30 mA electrolysis		100 %	90 min	–	[4]
DBD plasma treatment	5 mg/L TRA in 1 L solution operated in continuous flow mode	Continuous flow	93 %	60 min	0.056 min^{-1}	This work

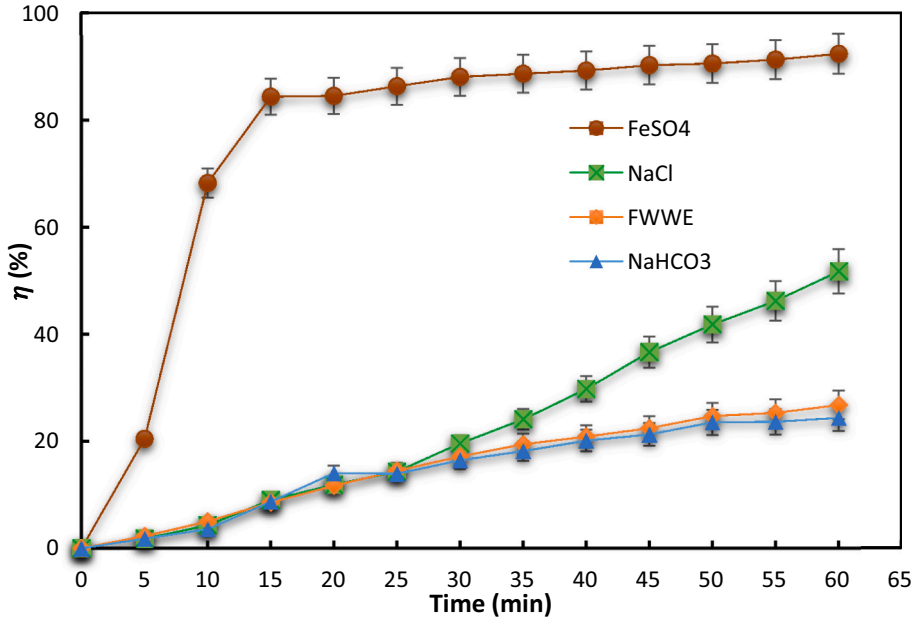

Fig. 7. Degradation of tramadol in different reaction solutions (initial TRA concentration: 5 mg/L; voltage: 8 kV).

increased with the pH of the treated solution [39], as well as another study on phenol [42]. The reason for this can be explained by the fact that under basic pH conditions, ozone is further decomposed into more powerful oxidants like hydroxyl radicals and superoxide ions [46]. However, this is not the case for this study as ozone is not the key driver for the removal of TRA.

3.4.4. *Effect of iron ions*

While Fe^{2+} was not detected in the wastewater effluent at specific sampling time, prior researches [47–50] have reported that the degradation efficiency of micropollutants contaminants with a plasma reactor can be improved by the addition of Fe^{2+} as a metal ion catalyst. This is because Fe^{2+} reacts with H_2O_2 in the reactor to produce hydroxyl radicals as described in Eqs. (15)–(17) [51]. Therefore, this study examined the possible effect of Fe^{2+} in the DBD tramadol treatment. To do this, $FeSO_4.7H_2O$ was added into the deionized solution of tramadol to potentially increase the oxidizing potential of generated H_2O_2 by its conversion into •OH from the Fenton reaction. Fig. 7 and Table S1 illustrate the effect of the addition of Fe^{2+} on the degradation of TRA. The experiment was performed at a concentration of 0.3 mg/L Fe^{2+} which represents the legal limit for wastewater discharge [52]. With the addition of iron, the degradation of tramadol was enhanced significantly such that in just 15 min, 84 % of the pollutant had been removed compared to 73 % recorded for the solution without iron. Also, after 60 min the rate constant of the Fe-enhanced solution was 0.061 min^{-1} compared to 0.056 min^{-1} for the synthetic solution. Unlike, the solution without iron, with Fe^{2+} the concentration of H_2O_2 was 1.18 mg/L in 20 min. This suggested that H_2O_2 was used up quickly during the process to facilitate the production of more •OH. Based on these results, it may be inferred that the presence of Fe^{2+} in TRA solution could potentially influence its degradation efficiency with DBD plasma. Also, considering that the concentration of iron in wastewater could vary per time and season, it is recommended that future studies try to consider the possible effect of Fe^{2+} variation.

$$Fe^{2+} + H_2O_2 \rightarrow Fe(OH)^{2+} + \dot{O}H \quad (15)$$

$$H_2O_2 + Fe(OH)^{2+} \rightarrow Fe^{2+} + HO_2^{\cdot} + H_2O \quad (16)$$

$$Fe(OH)^{2+} \rightarrow Fe^{2+} + \dot{O}H \quad (17)$$

3.5. *Toxicity investigation*

An investigation on the effect of plasma exposure on the toxicity of pre-treated and treated TRA solutions was conducted, as shown in Fig. 8. The assessment of TRA solution toxicity was based on the inhibition of *E. coli* growth, serving as an indicator of the solution's potential harm. It was observed that the untreated TRA solution showed clear inhibition zones on the agar plates, while the plasma-treated solution had no inhibition zones after 60 min. This indicated that the plasma-treated TRA solution was non-toxic. As a baseline for comparative analysis, a third plate containing solely deionized water was included as a control within the experiment. The observed zones, in this case, were similar to those of the plasma-treated plate in Fig. 8(b).

4. Conclusion

An investigation of tramadol degradation in deionized and final wastewater effluent matrices was carried out in this study with a newly developed water-falling dielectric barrier discharge reactor. Initially, the rector was optimized for applied voltage and initial concentration of the pollutant. An increase in voltage directly led to an increase in the concentration of the reactive species, which in turn improved the degradation of tramadol. Meanwhile, an increase in the concentration of the pollutant was a setback to the conversion process as the available molecules quickly scavenged the reactive species and inhibited further degradation. The optimum degradation of tramadol occurred at a combination of 8 kV and 5 mg/L. At these conditions, degradation efficiency and rate constant in deionized water were 93 % and 0.056 min^{-1}, respectively. Contrarily, in the final wastewater matrix, tramadol degradation reached only 27 % with 0.0056 min^{-1} rate constant. To elucidate this discrepancy, the authors investigated the effect of the significant radical scavengers present in the effluent solution through control experiments carried out in deionized water. Among all ions examined, CO_3^{2-} in deionized water exhibited the closest resemblance with the final wastewater effluent with a similar rate constant (0.0056 min^{-1}). This is because the HCO_3^- ion scavenged •OH radicals that could have oxidized the organic pollutant to generate CO_3^{-}• in the solution. Fenton reaction was also observed for the degradation of tramadol with a slightly higher degradation and kinetics than the TRA synthetic solution. Also, an increase in pH reduced the efficiency of the degradation. A

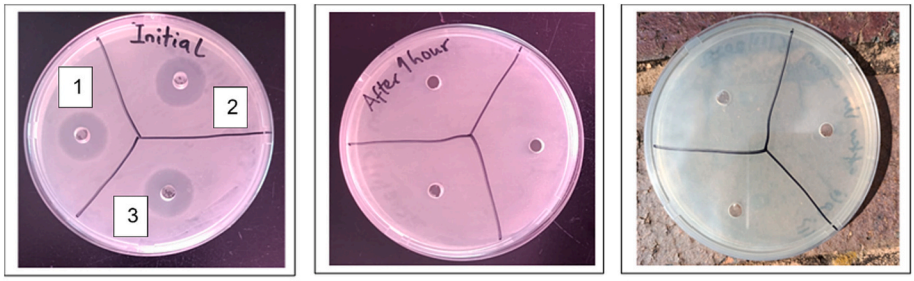

Fig. 8. Bioassay to study the antibacterial activity of TRA samples against Gram-negative *E. coli* strain. (a) Untreated tramadol solution with three zones of inhibition; (b) plasma-treated tramadol solution showing no inhibition zones; (c) is the control.

toxicity test was used to confirm that the plasma-treated solution did not affect a Gram-negative *E. coli*. Considering that the addition of inorganic compounds that act as radical scavengers change the properties of water and treatment performances, the effect of their concentration should be investigated in future studies.

CRediT authorship contribution statement

Samuel O. Babalola: Conceptualization, Investigation, Writing – review & editing. **Michael O. Daramola:** Supervision, Writing – review & editing. **Samuel A. Iwarere:** Supervision, Funding acquisition, Validation, Writing – review & editing.

Declaration of competing interest

The authors declare that they have no known competing financial interests or personal relationships that could have appeared to influence the work reported in this paper.

Samuel Ayodele Iwarere reports financial support was provided by The Royal Society.

Data availability

Data will be made available on request.

Acknowledgment

This research was supported by the Government of the United Kingdom through The Royal Society FLAIR award [FLR\R1\201683].

Appendix A. Supplementary data

Supplementary data to this article can be found online at https://doi.org/10.1016/j.jwpe.2023.104294.

References

[1] C.G. Daughton, Green Pharmacy | Mini-monograph cradle-to-cradle stewardship of drugs for minimizing their environmental disposition while promoting human health. II. Drug disposal, waste reduction, and future directions, Green Pharm. 111 (2003) 775–785, https://doi.org/10.1289/ehp.5948.

[2] A.C. Kondor, É. Molnár, A. Vancsik, T. Filep, J. Szeberényi, L. Szabó, et al., Occurrence and health risk assessment of pharmaceutically active compounds in riverbank filtrated drinking water, J. Water Process Eng. 41 (2021), https://doi.org/10.1016/j.jwpe.2021.102039.

[3] L. Radbruch, G. Glaeske, S. Grond, F. Münchberg, N. Scherbaum, E. Storz, et al., Topical review on the abuse and misuse potential of tramadol and tilidine in Germany, Subst. Abus. (2013) 37–41, https://doi.org/10.1080/08897077.2012.735216.

[4] C.L. Eversloh, M. Schulz, M. Wagner, T.A. Ternes, Electrochemical oxidation of tramadol in low-salinity reverse osmosis concentrates using boron-doped diamond anodes, Water Res. 2 (2014) 293–304, https://doi.org/10.1016/j.watres.2014.12.021.

[5] B.N. Patel, N. Sharma, M. Sanyal, P.S. Shrivastav, An accurate, rapid and sensitive determination of tramadol and its active metabolite O-desmethyltramadol in human plasma by LC – MS/MS, J. Pharm. Biomed. Anal. 49 (2009) 354–366, https://doi.org/10.1016/j.jpba.2008.10.030.

[6] P. Kostanjevecki, I. Petric, J. Loncar, T. Smital, M. Ahel, S. Terzic, Aerobic biodegradation of tramadol by pre-adapted activated sludge culture: cometabolic transformations and bacterial community changes during enrichment, Sci. Total Environ. 687 (2019) 858–866, https://doi.org/10.1016/j.scitotenv.2019.06.118.

[7] R. Bachour, O. Golovko, M. Kellner, J. Pohl, Behavioral effects of citalopram, tramadol, and binary mixture in zebrafish (*Danio rerio*) larvae, Chemosphere 238 (2020), 124587, https://doi.org/10.1016/j.chemosphere.2019.124587.

[8] F. Ložek, I. Kuklina, K. Grabicová, J. Kubec, M. Buřič, R. Grabic, et al., Behaviour and cardiac response to stress in signal crayfish exposed to environmental concentrations of tramadol, Aquat. Toxicol. 213 (2019), 105217, https://doi.org/10.1016/j.aquatox.2019.05.019.

[9] H.A.M. Soliman, A.E.D.H. Sayed, Poikilocytosis and tissue damage as negative impacts of tramadol on juvenile of Tilapia (Oreochromis niloticus), Environ. Toxicol. Pharmacol. 78 (2020), 103383, https://doi.org/10.1016/j.etap.2020.103383.

[10] P. Sehonova, L. Plhalova, J. Blahova, P. Berankova, V. Doubkova, M. Prokes, et al., The effect of tramadol hydrochloride on early life stages of fish, Environ. Toxicol. Pharmacol. 44 (2016) 151–157, https://doi.org/10.1016/j.etap.2016.05.006.

[11] R. Banaschik, H. Jablonowski, P.J. Bednarski, J.F. Kolb, Degradation and intermediates of diclofenac as instructive example for decomposition of recalcitrant pharmaceuticals by hydroxyl radicals generated with pulsed corona plasma in water, J. Hazard. Mater. 342 (2018) 651–660, https://doi.org/10.1016/j.jhazmat.2017.08.058.

[12] M.H.F. Graumans, W.F.L.M. Hoeben, M.F.P. van Dael, R.B.M. Anzion, F.G. M. Russel, P.T.J. Scheepers, Thermal plasma activation and UV/H2O2 oxidative degradation of pharmaceutical residues, Environ. Res. 195 (2021), 110884, https://doi.org/10.1016/j.envres.2021.110884.

[13] J. Zeng, B. Yang, X. Wang, Z. Li, X. Zhang, L. Lei, Degradation of pharmaceutical contaminant ibuprofen in aqueous solution by cylindrical wetted-wall corona discharge, Chem. Eng. J. 267 (2015) 282–288, https://doi.org/10.1016/j.cej.2015.01.030.

[14] L. Chandana, C. Subrahmanyam, Degradation and mineralization of aqueous phenol by an atmospheric pressure catalytic plasma reactor, J. Environ. Chem. Eng. 6 (2018) 3780–3786, https://doi.org/10.1016/j.jece.2016.11.014.

[15] A.N. Ghalwa, H.M. Abu-shawish, F.R. Zaggout, S.M. Saadeh, A.R. Al-dalou, A. A. Abou, Electrochemical degradation of tramadol hydrochloride: novel use of potentiometric carbon paste electrodes as a tracer, Arab. J. Chem. 7 (2014) 708–714, https://doi.org/10.1016/j.arabjc.2010.12.007.

[16] S.G. Zimmermann, A. Schmukat, M. Schulz, J. Benner, U. Von Gunten, T.A. Ternes, Kinetic and mechanistic investigations of the oxidation of tramadol by ferrate and ozone, Environ. Sci. Technol. 46 (2012) 876–884, https://doi.org/10.1021/es203348q.

[17] M. Cobo-Golpe, V. Fernandez-Fernandez, T. Arias, M. Ramil, R. Cela, I. Rodríguez, Comparison of UV, chlorination, UV-hydrogen peroxide and UV-chlorine processes for tramadol removal: kinetics study and transformation products identification, J. Environ. Chem. Eng. 10 (2022) 1–10, https://doi.org/10.1016/j.jece.2022.107854.

[18] M. Antonopoulou, I. Konstantinou, Photocatalytic degradation and mineralization of tramadol pharmaceutical in aqueous TiO2 suspensions: evaluation of kinetics, mechanisms and ecotoxicity, Appl. Catal. A Gen. 515 (2016) 136–143, https://doi.org/10.1016/j.apcata.2016.02.005.

[19] M. Antonopoulou, A. Thoma, F. Konstantinou, D. Vlastos, D. Hela, Assessing the human risk and the environmental fate of pharmaceutical tramadol, Sci. Total Environ. 710 (2020), https://doi.org/10.1016/j.scitotenv.2019.135396.

[20] F. Kazemi, H.A. Zamani, M.R. Abedi, M. Ebrahimi, Synthesis and comparison of three photocatalysts for degrading tramadol as an analgesic and widely used drug in water samples, Environ. Res. 114821 (2022), https://doi.org/10.1016/j.envres.2022.114821.

[21] H. Monteil, N. Oturan, Y. Péchaud, M.A. Oturan, Electro-Fenton treatment of the analgesic tramadol: kinetics, mechanism and energetic evaluation, Chemosphere 247 (2020), https://doi.org/10.1016/j.chemosphere.2020.125939.

[22] B. Jiang, J. Zheng, S. Qiu, M. Wu, Q. Zhang, Z. Yan, et al., Review on electrical discharge plasma technology for wastewater remediation, Chem. Eng. J. 236 (2014) 348–368, https://doi.org/10.1016/j.cej.2013.09.090.
[23] Y. Cui, J. Cheng, Q. Chen, Z. Yin, The types of plasma reactors in wastewater treatment, IOP Conf. Ser. Earth Environ. Sci. 208 (2018), https://doi.org/10.1088/1755-1315/208/1/012002.
[24] M.A. Malik, Water purification by plasmas: which reactors are most energy efficient? Plasma Chem. Plasma Process. 30 (2010) 21–31, https://doi.org/10.1007/s11090-009-9202-2.
[25] J.E. Foster, Plasma-based water purification: challenges and prospects for the future, Phys. Plasmas 24 (2017) 0–16, https://doi.org/10.1063/1.4977921.
[26] S.M. Allabakshi, P.S.N.S.R. Srikar, R.K. Gangwar, S.M. Maliyekkal, Feasibility of surface dielectric barrier discharge in wastewater treatment: spectroscopic modeling, diagnostic, and dye mineralization, Sep. Purif. Technol. 296 (2022) 121344, https://doi.org/10.1016/j.seppur.2022.121344.
[27] M. Sato, T. Ohgiyama, J.S. Clements, Formation of chemical species and their effects on microorganisms using a pulsed high-voltage discharge in water, IEEE Trans. Ind. Appl. 32 (1996) 106–112, https://doi.org/10.1109/28.485820.
[28] S. Karoui, W.A. Saoud, A. Ghorbal, F. Fourcade, A. Amrane, A.A. Assadi, Intensification of non-thermal plasma for aqueous ciprofloxacin degradation: optimization study, mechanisms, and combined plasma with photocatalysis, J. Water Process Eng. 50 (2022), 103207, https://doi.org/10.1016/j.jwpe.2022.103207.
[29] Z. Machala, M. Janda, K. Hensel, I. Jedlovský, L. Leštinská, V. Foltin, et al., Emission spectroscopy of atmospheric pressure plasmas for bio-medical and environmental applications, J. Mol. Spectrosc. 243 (2007) 194–201, https://doi.org/10.1016/j.jms.2007.03.001.
[30] T. Zhang, R. Zhou, P. Wang, A. Mai-prochnow, R. Mcconchie, W. Li, et al., Degradation of cefixime antibiotic in water by atmospheric plasma bubbles: performance, degradation pathways and toxicity evaluation, Chem. Eng. J. 421 (2021), 127730, https://doi.org/10.1016/j.cej.2020.127730.
[31] X. Lu, G.V. Naidis, M. Laroussi, S. Reuter, D.B. Graves, K. Ostrikov, Reactive species in non-equilibrium atmospheric-pressure plasmas: generation, transport, and biological effects, Phys. Rep. 630 (2016) 1–84, https://doi.org/10.1016/j.physrep.2016.03.003.
[32] A.S. Bansode, S.E. More, E.A. Siddiqui, S. Satpute, A. Ahmad, S.V. Bhoraskar, et al., Effective degradation of organic water pollutants by atmospheric non-thermal plasma torch and analysis of degradation process, Chemosphere 167 (2017) 396–405, https://doi.org/10.1016/j.chemosphere.2016.09.089.
[33] M. Magureanu, F. Bilea, C. Bradu, D. Hong, A review on non-thermal plasma treatment of water contaminated with antibiotics, J. Hazard. Mater. 417 (2021), https://doi.org/10.1016/j.jhazmat.2021.125481.
[34] S. Meropoulis, S. Giannoulia, S. Skandalis, G. Rassias, C.A. Aggelopoulos, Key-study on plasma-induced degradation of cephalosporins in water: process optimization, assessment of degradation mechanisms and residual toxicity, Sep. Purif. Technol. 298 (2022) 121639, https://doi.org/10.1016/j.seppur.2022.121639.
[35] Z. Li, Y. Wang, H. Guo, S. Pan, C. Puyang, Y. Su, et al., Insights into water film DBD plasma driven by pulse power for ibuprofen elimination in water: performance, mechanism and degradation route, Sep. Purif. Technol. 277 (2021) 119415, https://doi.org/10.1016/j.seppur.2021.119415.
[36] D. Nikitin, B. Kaur, S. Preis, N. Dulova, Persulfate contribution to photolytic and pulsed corona discharge oxidation of metformin and tramadol in water, Process. Saf. Environ. Prot. 165 (2022) 22–30, https://doi.org/10.1016/j.psep.2022.07.002.
[37] S. Ghazouani, F. Boujelbane, D. Jellouli, B. Van Der Bruggen, Removal of tramadol hydrochloride, an emerging pollutant, from aqueous solution using gamma irradiation combined by nanofiltration, Process. Saf. Environ. Prot. 159 (2022) 442–451, https://doi.org/10.1016/j.psep.2022.01.005.
[38] S. Wales, B. Kasprzyk-hordern, R.M. Dinsdale, A.J. Guwy, The occurrence of pharmaceuticals, personal care products, endocrine disruptors and illicit drugs in surface water in South Wales, UK, Water Res. 42 (2008) 3498–3518, https://doi.org/10.1016/j.watres.2008.04.026.
[39] S.P. Rong, Y.B. Sun, Z.H. Zhao, Degradation of sulfadiazine antibiotics by water falling film dielectric barrier discharge, Chin. Chem. Lett. 25 (2014) 187–192, https://doi.org/10.1016/j.cclet.2013.11.003.
[40] M. Muthukumar, N. Selvakumar, Studies on the effect of inorganic salts on decolouration of acid dye effluents by ozonation, Dyes Pigments 62 (2004) 221–228, https://doi.org/10.1016/j.dyepig.2003.11.002.
[41] D.R. Merouani, F. Abdelmalek, F. Taleb, M. Martel, A. Semmoud, A. Addou, Plasma treatment by gliding arc discharge of dyes/dye mixtures in the presence of inorganic salts, Arab. J. Chem. 8 (2015) 155–163, https://doi.org/10.1016/j.arabjc.2011.01.034.
[42] E. Marotta, E. Ceriani, M. Schiorlin, C. Ceretta, C. Paradisi, Comparison of the rates of phenol advanced oxidation in deionized and tap water within a dielectric barrier discharge reactor, Water Res. 46 (2012) 6239–6246, https://doi.org/10.1016/j.watres.2012.08.022.
[43] L. Wojnárovits, T. Tóth, E. Takács, Rate constants of carbonate radical anion reactions with molecules of environmental interest in aqueous solution: a review, Sci. Total Environ. 717 (2020) 1–24, https://doi.org/10.1016/j.scitotenv.2020.137219.
[44] S. Canonica, T. Kohn, M. Mac, F.J. Real, J. Wirz, U. von Gunten, Photosensitizer method to determine rate constants for the reaction of carbonate radical with organic compounds, Environ. Sci. Technol. 39 (2005) 9182–9188, https://doi.org/10.1021/es051236b.
[45] J. Hoigne, H. Bader, The role of hydroxyl radical reactions in oxidation processes in aqueous solutions, Water Res. 10 (1976) 377–386, https://doi.org/10.1016/0043-1354(76)90055-5.
[46] H. Zeghioud, P. Nguyen-Tri, L. Khezami, A. Amrane, A.A. Assadi, Review on discharge plasma for water treatment: mechanism, reactor geometries, active species and combined processes, J. Water Process Eng. 38 (2020), 101664, https://doi.org/10.1016/j.jwpe.2020.101664.
[47] K. Hikmat, H. Aziz, H. Miessner, S. Mueller, D. Kalass, D. Moeller, et al., Degradation of pharmaceutical diclofenac and ibuprofen in aqueous solution, a direct comparison of ozonation, photocatalysis, and non-thermal plasma, Chem. Eng. J. 313 (2017) 1033–1041, https://doi.org/10.1016/j.cej.2016.10.137.
[48] K. Hsieh, H. Wang, B.R. Locke, Analysis of a gas-liquid film plasma reactor for organic compound oxidation, J. Hazard. Mater. 317 (2016) 188–197, https://doi.org/10.1016/j.jhazmat.2016.05.053.
[49] D.B. Miklos, C. Remy, M. Jekel, K.G. Linden, J.E. Drewes, U. Hübner, Evaluation of advanced oxidation processes for water and wastewater treatment – a critical review, Water Res. 139 (2018) 118–131, https://doi.org/10.1016/j.watres.2018.03.042.
[50] S. Slamani, F. Abdelmalek, M.R. Ghezzar, A. Addou, Initiation of Fenton process by plasma gliding arc discharge for the degradation of paracetamol in water, J. Photochem. Photobiol. A Chem. 359 (2018) 1–10, https://doi.org/10.1016/j.jphotochem.2018.03.032.
[51] Y. Sun, J.J. Pignatello, Photochemical reactions involved in the total mineralization of 2,4-D by Fe3+/H202/UV, Environ. Sci. Technol. 27 (1993) 304–310, https://doi.org/10.1021/es00039a010.
[52] B.E. Molewa, National Water Act 36 of 1998 vol. 1998, 2013. Pretoria.